Low-Complexity Iterative Joint Source-Channel Decoding for Variable-Length Encoded Markov Sources

Ragnar Thobaben and Jörg Kliewer, Senior Member, IEEE

Abstract—In this paper, we present a novel packetized bit-level decoding algorithm for variable-length encoded Markov sources, which calculates reliability information for the decoded bits in the form of a posteriori probabilities (APPs). An interesting feature of the proposed approach is that symbol-based source statistics in the form of the transition probabilities of the Markov source are in [2] and [3] consider a rst-order Markov source model; the remaining approaches assume uncorrelated sources.

In [8], a symbol-level trellis representation for uncorrelated variable-length encoded data packets is presented, where the Bahl–Cocke–Jelinek–Raviv (BCJR) algorithm [9] is used as an a posteriori probability (APP) decoder. The soft outputs for the source symbols are then used in an iterative source-channel decoding (ISCD) scheme. This approach is extended in [10] and [11] to first-order Gauss–Markov sources, where the residual source correlation is additionally exploited in the decoding process. Especially, in [11], a 3-D trellis representation is proposed, which is capable of exploiting all possible source redundancy and leads to optimal symbol-based APP decoding. However, the used symbol-level trellis has the drawback that for long source packets, the number of trellis states increases drastically, such that the decoding operation becomes computationally quite expensive.

On the other hand, a bit-level trellis is proposed in [12], which has a constant number of states only depending on the VLC tree depth, and thus does not lead to a complexity problem for long blocks of source data. This trellis is used for iterative VLC APP decoding in [13], where robust VLCs are selected based on their distance properties. In [14], an iterative decoder for a variable-length encoded source being serially concatenated

with a turbo code is proposed by merging the bit-level trellis from [12] with the trellis for one constituent channel code. The decoding is then carried out iteratively between an APP decoder working on the combined trellis and an APP decoder for the remaining constituent channel code. A related approach has been presented in [15], where bit-based a priori information from Huffman codewords is used in the turbo decoding process. All these methods only consider uncorrelated source samples, and do not take Markov sources into account. In [16], the joint source-channel decoding problem for variable-length encoded first-order Markov sources is considered within the framework of Bayesian networks. Here, the authors show that in contrast to the VLC decoding approach presented in this paper, the interpretation of APP decoding as a message-passing problem also allows performing the decoding of the Markov source and VLC source decoding separately.

In this paper, we assume that correlated source indices are generated by quantizing a first-order autoregressive [AR(1)] source process. The quantized indexes can be modeled as a first-order Markov process, which serves as a good model for the residual source redundancy inherent in quantized and compressed data sequences at the output of many source encoders. The residual interframe correlation between (quantized) speech codec parameters for adjacent time instants or frames is, e.g., examined in [17]–[20]. In [17], it is stated for the 4.6 kb/s U.S. Federal Standard 1016 (FS 1016) speech codec that approximately one-third of the bits obtained after quantizing the line spectral frequencies (LSFs) are redundant, when in addition to the interframe redundancy, also the parameter correlation within one frame is considered. Recently, for the gain and pitch parameters of the 2.4 kb/s mixed-excitation linear predictive (MELP) speech-compression algorithm, it is observed in [18] that 40%–50% of the overall number of bits in a frame are redundant due to additional interframe correlation, besides the distribution-based correlation of the parameter indexes. According to [19] and [20], for the global system for mobile communications (GSM) full-rate speech codec, interframe correlation results in up to 28% of redundant bits for the log area ratio (LAR) and regular pulse excitation (RPE) block amplitude parameters. Similar observations also apply to MPEG audio compression, where a strong interframe parameter correlation can be observed, e.g., for the scale-factor parameters [21]. From all these examples, we can see that even for state-of-the-art source coding schemes, source parameter correlation in time may be fairly high, and thus, it seems reasonable to exploit these dependencies for additional error protection. As another aspect, in [22], the authors demonstrate for the IS-641 speech codec that intentionally inserting some residual source redundancy by less powerful source encoding may result in a higher error resilience. These two facts essentially motivate the consideration of first-order Markov source models in this paper.

In the following, we present a joint source-channel decoding approach for packetized variable-length encoded correlated source data, based on the bit-level VLC trellis from [12]. As a novelty, we show for a first-order Markov source that by using an appropriately adapted soft-input soft-output (SISO) decoder, the available source correlation can be exploited in the VLC decoder with only a slight increase in complexity, compared
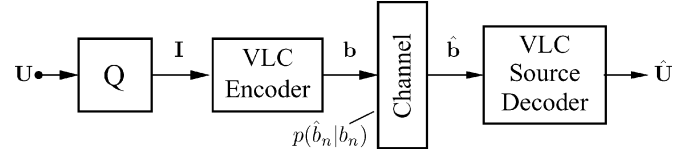

Fig. 1. Model of the transmission system.

with the approach in [13]. When the resulting variable-length encoded bitstream is additionally protected by a channel code, the proposed bit-level VLC decoder can be used as constituent decoder in an ISCD scheme. The second part of the paper discusses the optimization of the overall transmission system by selecting a suitable channel code via an extrinsic information transfer (EXIT) chart analysis [23]. We demonstrate that by inserting explicit redundancy in the form of reversible VLCs (RVLCs) [24] with a free distance of two, good recursive systematic convolutional (RSC) rate-one channel codes with low memory can be found. Especially when residual source index correlations are present, a robust transmission system with increased bandwidth efficiency is obtained, compared with previously published serially concatenated approaches [8], [10], [13]–[15] with channel codes having code rates smaller than one.

This paper is organized as follows. In Section II, we introduce the underlying transmission scenario and the used VLC bit-level trellis. Then, using this trellis representation, a new APP VLC decoder is derived by a modification of the classical BCJR algorithm. This approach exploits the index-transition probabilities for a first-order Markov source as additional a priori information in both the forward and backward recursion of the decoding algorithm. Section III addresses the case of an additional FEC. Based on an EXIT chart analysis for the corresponding iterative source-channel decoder, we perform a code search over a suitable subset of rate-1 codes generated by puncturing from a high-rate RSC code in order to obtain a good matching code for a given RVLC. Finally, Section IV discusses the overall performance of the simulated transmission system, and compares it with a transmission system employing both Huffman codes and turbo-like FEC codes.

II. APP SOURCE DECODING

A. Transmission Model

The derivation of the APP source decoder is based on the transmission system shown in Fig. 1, where a packet of K correlated source symbols is given by $\mathbf{U} = [U_1, U_2, \ldots, U_K]$. A subsequent (vector) quantization of source symbols U_k results in indexes $I_k \in \mathcal{I}$ from the finite alphabet $\mathcal{I} = \{0, 1, \ldots, 2^M - 1\}$ represented with M bits. Due to delay and complexity constraints for the quantization stage, a residual index correlation remains in the index vector $\mathbf{I}$, which is modeled as a first-order (stationary) Markov process with index-transition probabilities $P(I_0 = \lambda | I_{-1} = \mu)$ for $\lambda, \mu \in \mathcal{I}$. The quantization stage is followed by a VLC encoder, which maps a fixed-length index I_k to a variable-length bit vector $\mathbf{c}(\lambda) = \mathcal{C}(I_k = \lambda)$ of length $l(\mathbf{c}(\lambda))$ using the prefix code $\mathcal{C}$. The output of the VLC encoder is given by the binary sequence $\mathbf{b} = [b_1, b_2, \ldots, b_N]$ of length N, where $b_n \in \{0, 1\}$ represents a single bit at bit index n. The
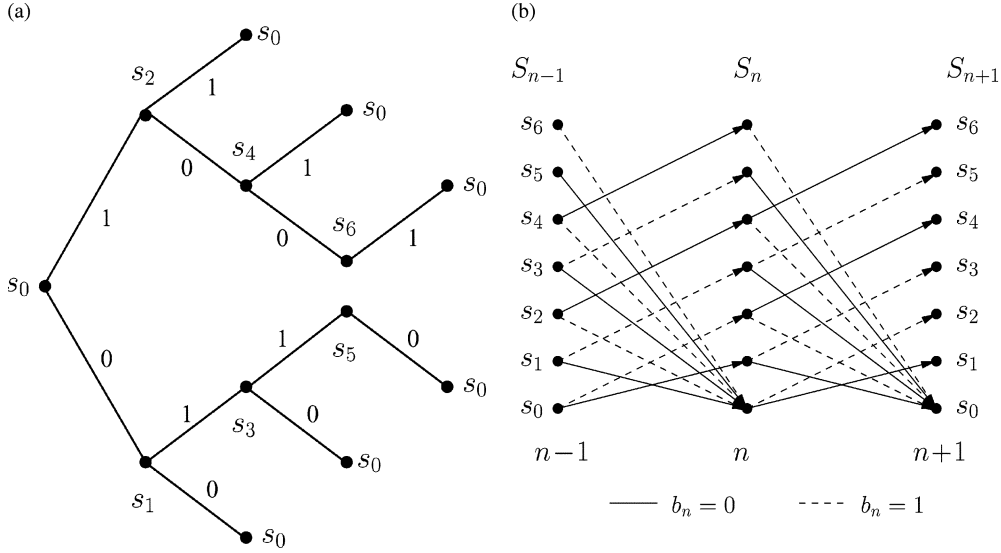
Fig. 2.   (a) Code tree and (b) trellis representation for the RVLC $\mathcal{C} = \{\mathbf{c}(0) = [11], \mathbf{c}(1) = [00], \mathbf{c}(2) = [101], \mathbf{c}(3) = [010], \mathbf{c}(4) = [1001], \mathbf{c}(5) = [0110]\}$.

transmission of one bit over the memoryless channel character-ized by the probability density function (PDF) $p(\hat{b}_n|b_n)$ leads to a soft-bit $\hat{b}_n \in \mathbb{R}$ at the channel output.

B. Trellis Representation

Since a VLC encoder can be seen as a finite-state machine with binary output, all possible output sequences $\mathbf{b}$ can be de-scribed in a trellis diagram. A quite simple trellis representa-tion is proposed in [12], where the VLC trellis is derived from the corresponding code tree by mapping each node to a spe-cific trellis state. The root node and all leaf nodes are mapped to the same trellis state, since in a sequence of codewords, every leaf becomes the root of the tree for the next codeword. Each transition from state S_{n-1} to state S_n is caused by a single bit $b_n \in \{0, 1\}$ at time instant $n = 1, \ldots, N$ at the output of the VLC encoder. An example is given in Fig. 2, where the code tree and a trellis segment for the RVLC

$$\mathcal{C} = \{\mathbf{c}(0) = [11], \mathbf{c}(1) = [00], \mathbf{c}(2) = [101], \mathbf{c}(3) = [010],$$
$$\mathbf{c}(4) = [1001], \mathbf{c}(5) = [0110]\} \quad (1)$$

is shown. In the following, we denote the set of all N_s trellis states as $\mathcal{S} = \{s_0, \ldots, s_{N_s-1}\}$, where the s_κ, $\kappa = 0, \ldots, N_s-1$, represent the individual state hypotheses. Furthermore, the bit position for the root state is denoted with ν, $\nu \in \{0, \ldots, N\}$, and for the sake of brevity, its hypothesis $S_\nu = s_0$ is written as $S_\nu = 0$ in the remainder of this paper.

Due to the unique relationship between the VLC tree and VLC trellis, every state $S_n = \sigma$, $\sigma \in \mathcal{S}$, is associated with a certain codeword prefix written as $\mathbf{c}_{[0,\ldots,\sigma]}$, or equiva-lently, with a state sequence $[S_\nu, \ldots, S_n] = [0, \ldots, \sigma]$. This corresponds to a certain subset of codewords $\mathcal{P}_\sigma = \{\lambda \in \mathcal{I} | \mathbf{c}_{[0,\ldots,\sigma]}$ is the prefix of $\mathbf{c}(\lambda)\}$, where $\mathbf{c}_{[0,\ldots,\sigma]}$ represents the VLC codeword prefix associated with the state $S_n = \sigma$. For the case $S_n = \sigma = 0$, the prefix $\mathbf{c}_{[0]}$ is empty and $\mathcal{P}_0 = \mathcal{I}$. Corre-spondingly, for each state transition from state $S_{n-1} = \sigma_1$ to state $S_n = \sigma_2$, with $\sigma_1, \sigma_2 \in \mathcal{S}$, which is due to the bit $b_n = i$, $i \in \{0, 1\}$, a similar subset $\mathcal{P}_{\sigma_1,\sigma_2,i} = \{\lambda \in \mathcal{I} | \mathbf{c}_{[0,\ldots,\sigma_1\sigma_2]}$

$= [\mathbf{c}_{[0,\ldots,\sigma_1]}i]$ is the prefix of $\mathbf{c}(\lambda)\}$ can be defined. As an example, the subset corresponding to state $S_n = s_4$ in Fig. 2 is given by $\mathcal{P}_{s_4} = \{2, 4\}$, and the corresponding prefix is given by $\mathbf{c}_{[0,\ldots,s_4]} = [10]$.

C. Derivation of the APPs

In the following, we derive a SISO decoding algorithm which delivers reliability information for the source bits $b_n = i$, $i \in \{0, 1\}$, in the form of APPs $P(b_n = i|\hat{\mathbf{b}})$. As a new result, we show that it is possible to exploit the first-order Markov prop-erty of the quantization indexes modeled by the index-transition probabilities $P(I_0 = \lambda|I_{-1} = \mu)$ as a priori information in a bit-level decoding algorithm, based on the VLC trellis represen-tation from above.

By employing the VLC trellis representation of the bit se-quence $\mathbf{b}$, the APPs $P(b_n = i|\hat{\mathbf{b}})$ can be expressed as a mar-ginal distribution of the APPs for the state transitions from state $S_{n-1} = \sigma_1$ to state $S_n = \sigma_2$ corresponding to the bit $b_n = i$

$$P(b_n = i|\hat{\mathbf{b}}) = \sum_{\sigma_1 \in \mathcal{S}} \sum_{\sigma_2 \in \mathcal{S}} P(S_{n-1} = \sigma_1, b_n = i, S_n = \sigma_2|\hat{\mathbf{b}}).$$
$$(2)$$

Following the derivation of the classical BCJR algorithm [9], [25], the APPs for the state transitions $P(S_{n-1} = \sigma_1, b_n = i, S_n = \sigma_2|\hat{\mathbf{b}})$ can further be factorized into three terms, namely, $\alpha_{n-1}(\sigma_1)$, $\beta_n(\sigma_2)$, and $\gamma_n(i, \sigma_2, \sigma_1)$, and a normalization con-stant $p(\hat{\mathbf{b}})$ according to

$$P(S_{n-1} = \sigma_1, b_n = i, S_n = \sigma_2|\hat{\mathbf{b}})$$
$$= \frac{1}{p(\hat{\mathbf{b}})} \cdot \underbrace{p\left(\hat{\mathbf{b}}_{n+1}^N|S_n = \sigma_2, \hat{\mathbf{b}}_1^n\right)}_{\beta_n(\sigma_2)}$$
$$\cdot \underbrace{p\left(\hat{b}_n, b_n = i, S_n = \sigma_2|S_{n-1} = \sigma_1, \hat{\mathbf{b}}_1^{n-1}\right)}_{\gamma_n(i, \sigma_2, \sigma_1)}$$
$$\cdot \underbrace{p\left(S_{n-1} = \sigma_1, \hat{\mathbf{b}}_1^{n-1}\right)}_{\alpha_{n-1}(\sigma_1)} \quad (3)$$

where, e.g., $\hat{\mathbf{b}}_{n+1}^{N}$ specifies the subsequence $\hat{\mathbf{b}}_{n+1}^{N} = [\hat{b}_{n+1}, \hat{b}_{n+2}, \ldots, \hat{b}_{N}]$. In contrast to the classical BCJR algorithm, the γ and β terms in (3) are now conditioned on the channel observations $\hat{\mathbf{b}}_{1}^{n-1}$ and $\hat{\mathbf{b}}_{1}^{n}$, respectively. This is due to the fact that, e.g., for the β term, $\hat{\mathbf{b}}_{n+1}^{N}$ and $\hat{\mathbf{b}}_{1}^{n}$ can not be assumed as independent by conditioning on a certain state $S_n = \sigma_2$, since mutual index correlations are present in the sequence of quantization indexes $\mathbf{I}$. Correspondingly, we obtain a modified forward recursion for the derivation of both $\alpha_{n-1}(\sigma_1)$ and $\gamma_n(i, \sigma_2, \sigma_1)$, and a modified backward recursion for the term $\beta_n(\sigma_2)$. In the following, the derivations for both recursions are presented for the special case of first-order Markov sources.

1) Forward Recursion: The modified forward recursion $\alpha_n(\sigma_2)$ is given as

$$\alpha_n(\sigma_2) = \sum_{\sigma_1 \in \mathcal{S}} \sum_{i=0}^{1} \gamma_n(i, \sigma_2, \sigma_1) \alpha_{n-1}(\sigma_1), \quad \alpha_0(0) = 1 \quad (4)$$

and it differs from the classical BCJR forward recursion [9] due to the modified γ term from (3)

$$\gamma_n(i, \sigma_2, \sigma_1) = p(\hat{b}_n | b_n = i) \cdot P\left(b_n = i, S_n = \sigma_2 | S_{n-1} = \sigma_1, \hat{\mathbf{b}}_1^{n-1}\right). \quad (5)$$

The first term on the right-hand side (RHS) of (5) corresponds to the soft output of the transmission channel for the bit $b_n = i$. The second term specifies the probability of a transition from state $S_{n-1} = \sigma_1$ to state $S_n = \sigma_2$, which is due to bit $b_n = i$, conditioned on the previously received channel observations $\hat{\mathbf{b}}_1^{n-1}$. This term allows us to include the statistics of the first-order Markov source model as additional a priori information in the forward recursion, as we show in the following.

In a first step, the probability for a state transition $P(b_n = i, S_n = \sigma_2 | S_{n-1} = \sigma_1, \hat{\mathbf{b}}_1^{n-1})$ in (5) is expressed by symbol-based probabilities of codewords which are from the subsets $\mathcal{P}_{\sigma_1}$ and $\mathcal{P}_{\sigma_1, \sigma_2, i}$, associated with the current trellis state $S_{n-1} = \sigma_1$ and the transition from state $S_{n-1} = \sigma_1$ to state $S_n = \sigma_2$, respectively. These subsets define a common prefix $\mathbf{c}_{[0, \ldots, \sigma_1]}$, starting at the root state $S_\nu = 0$ with $\nu = n - 1 - l(\mathbf{c}_{[0, \ldots, \sigma_1]})$. Thus, we can replace the hypotheses for the trellis states and the affected bit b_n in the second term on the RHS of (5) with the hypotheses for the associated subsets of the codewords $\mathcal{P}_{\sigma_1}$ and $\mathcal{P}_{\sigma_1, \sigma_2, i}$ and the root state $S_\nu = 0$ as

$$P\left(b_n = i, S_n = \sigma_2 | S_{n-1} = \sigma_1, \hat{\mathbf{b}}_1^{n-1}\right)$$
$$= P\left(I_0 \in \mathcal{P}_{\sigma_1, \sigma_2, i} | I_0 \in \mathcal{P}_{\sigma_1}, S_\nu = 0, \hat{\mathbf{b}}_1^{n-1}\right). \quad (6)$$

Herein, the VLC codewords are indexed by the current quantization index, which is represented by I_0. Since in (6), the trellis states $S_{n-1} = \sigma_1$ and $S_n = \sigma_2$ represent a pair of ascending trellis states, it follows that $\mathcal{P}_{\sigma_1, \sigma_2, i} \subset \mathcal{P}_{\sigma_1}$. By using this result, and by applying the definition of the conditional probability to the RHS of (6), we obtain

$$P\left(I_0 \in \mathcal{P}_{\sigma_1, \sigma_2, i} | I_0 \in \mathcal{P}_{\sigma_1}, S_\nu = 0, \hat{\mathbf{b}}_1^{n-1}\right)$$
$$= \frac{P\left(I_0 \in \mathcal{P}_{\sigma_1, \sigma_2, i} | S_\nu = 0, \hat{\mathbf{b}}_1^{n-1}\right)}{P\left(I_0 \in \mathcal{P}_{\sigma_1} | S_\nu = 0, \hat{\mathbf{b}}_1^{n-1}\right)}. \quad (7)$$

The conditional probabilities in (7) can now be expressed as marginal distributions of the probabilities for those VLC codewords which start at the root state $S_\nu = 0$, conditioned on the observations $\hat{\mathbf{b}}_1^{n-1}$. Therefore, let the set $\mathcal{P}$ generically denote the subset $\mathcal{P}_{\sigma_1}$ or $\mathcal{P}_{\sigma_1, \sigma_2, i}$. The probabilities for the subsets of the VLC codewords in (7) are then determined as

$$P\left(I_0 \in \mathcal{P} | S_\nu = 0, \hat{\mathbf{b}}_1^{n-1}\right) = \sum_{\lambda \in \mathcal{P}} P\left(I_0 = \lambda | S_\nu = 0, \hat{\mathbf{b}}_1^{n-1}\right). \quad (8)$$

The symbol probabilities $P(I_0 = \lambda | S_\nu = 0, \hat{\mathbf{b}}_1^{n-1})$ in (8) can furthermore be decomposed for $\lambda \in \mathcal{P}_{\sigma_1}, \mathcal{P}_{\sigma_1, \sigma_2, i}$ with the normalization factor C as

$$P\left(I_0 = \lambda | S_\nu = 0, \hat{\mathbf{b}}_1^{n-1}\right) = \frac{1}{C} \cdot p\left(\hat{\mathbf{b}}_{\nu+1}^{n-1} | \mathbf{c}_{[0, \ldots, \sigma_1]}\right)$$
$$\cdot P\left(I_0 = \lambda | S_\nu = 0, \hat{\mathbf{b}}_1^{\nu}\right). \quad (9)$$

The first term in (9) takes the current channel observations $\hat{\mathbf{b}}_{\nu+1}^{n-1}$ for the prefix $\mathbf{c}_{[0, \ldots, \sigma_1]}$ into account. The second term represents the conditional probability for the VLC codeword $\mathbf{c}(I_0 = \lambda)$ at bit position ν, which is conditioned on the previous observations $\hat{\mathbf{b}}_1^{\nu}$. By inserting (7)–(9) in (6), we can now state the desired relation between the state-transition probability in (5) and the symbol probabilities $P(I_0 = \lambda | S_\nu = 0, \hat{\mathbf{b}}_1^{\nu})$ as

$$P\left(b_n = i, S_n = \sigma_2 | S_{n-1} = \sigma_1, \hat{\mathbf{b}}_1^{n-1}\right) = \frac{1}{C(\sigma_1)}$$
$$\cdot \sum_{\lambda \in \mathcal{P}_{\sigma_1, \sigma_2, i}} P\left(I_0 = \lambda | S_\nu = 0, \hat{\mathbf{b}}_1^{\nu}\right) \quad (10)$$

with $\nu = n - 1 - l(\mathbf{c}_{[0, \ldots, \sigma_1]})$ and the normalization factor

$$C(\sigma_1) = \sum_{\lambda \in \mathcal{P}_{\sigma_1}} P\left(I_0 = \lambda | S_\nu = 0, \hat{\mathbf{b}}_1^{\nu}\right).$$

Note that the normalization factor C from (9), and also the conditional PDFs $p(\hat{\mathbf{b}}_{\nu+1}^{n-1} | \mathbf{c}_{[0, \ldots, \sigma_1]})$ are canceled in (10). This is due to the fact that all VLC codewords associated with both the sets $\mathcal{P}_{\sigma_1}$ and $\mathcal{P}_{\sigma_1, \sigma_2, i}$ have the same prefix for the first $(n - \nu - 1)$ bits.

The derivation of (10) is illustrated in Fig. 3 for a trellis segment of the RVLC given in (1), and a state transition from state $S_{n-1} = s_2$ to state $S_n = s_4$ affected by bit $b_n = 0$ at bit position n.

In order to use the index-transition probabilities $P(I_0 = \lambda | I_{-1} = \mu)$ as a priori information for APP decoding, the conditional probability $P(I_0 = \lambda | S_\nu = 0, \hat{\mathbf{b}}_1^{\nu})$ in (10) can now be written as

$$P\left(I_0 = \lambda | S_\nu = 0, \hat{\mathbf{b}}_1^{\nu}\right) = \sum_{\mu=0}^{2^M - 1} P(I_0 = \lambda | I_{-1} = \mu)$$
$$\cdot P\left(I_{-1} = \mu | S_\nu = 0, \hat{\mathbf{b}}_1^{\nu}\right). \quad (11)$$

The last missing term to be expressed with known quantities is the probability $P(I_{-1} = \mu | S_\nu = 0, \hat{\mathbf{b}}_1^{\nu})$ of the previous codeword $\mathbf{c}(\mu)$ which corresponds to the index $I_{-1} = \mu$ and ends at bit position ν in (11). Due to the fact that the trellis branch specified by the triple $(S_{\nu-1} = \sigma_0, S_\nu = 0, b_\nu = i)$, $\sigma_0 \in \mathcal{S}$ uniquely identifies the trellis path associated with the source index $I_{-1} = \mu$, $\mu \in \mathcal{I}$ at the previous index position, the hypothesis $I_{-1} = \mu$ may be replaced with $b_\nu = i(\mu)$ and
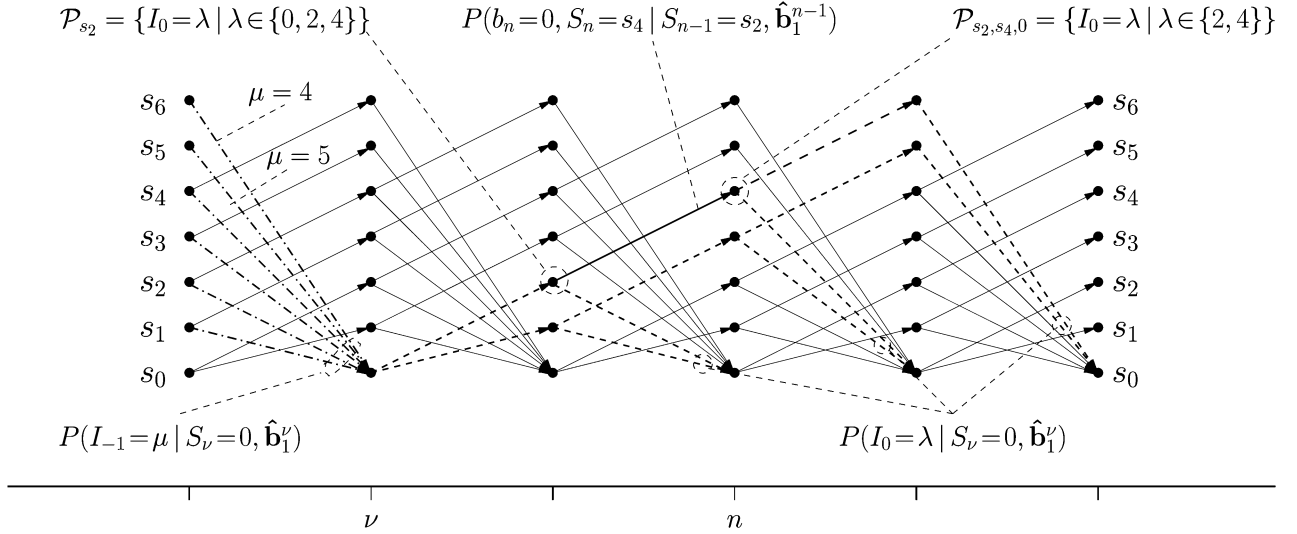
Fig. 3.   Forward recursion: derivation of the probability $P(b_n = i, S_n = \sigma_2 | S_{n-1} = \sigma_1, \hat{\mathbf{b}}_1^{n-1})$ from (5) for a state transition $(S_{n-1} = s_2, S_n = s_4, b_n = 0)$ and the RVLC example in (1).

$S_{\nu-1} = \sigma_0(\mu)$, which now depend on μ (see Fig. 3, e.g., for $\mu = 4, 5$). We thus obtain the expression

$$P\left(I_{-1} = \mu | S_\nu = 0, \hat{\mathbf{b}}_1^\nu\right)$$
$$= P\left(b_\nu = i(\mu), S_{\nu-1} = \sigma_0(\mu) | S_\nu = 0, \hat{\mathbf{b}}_1^\nu\right)$$
$$= \frac{1}{\alpha_\nu(0)} \cdot \gamma_\nu\left(i(\mu), 0, \sigma_0(\mu)\right) \cdot \alpha_{\nu-1}\left(\sigma_0(\mu)\right) \quad (12)$$

where the term $\alpha_\nu(0)$ serves as a normalization factor, depending on the bit position ν for the root state. Finally, combining (5), (10), (11), and (12) leads to a modified expression for the γ term, compared with the classical BCJR algorithm, which allows us to exploit the residual source correlation for additional error protection in the forward recursion (4).

2) Backward Recursion: The last missing quantity in (3) is given by the β term, which differs from the classical BCJR APP decoding approach [9] due to the dependency on the previous channel observations $\hat{\mathbf{b}}_1^n$. In the following, we show that the term $\beta_n(\sigma_2)$ can be obtained as a marginal distribution of a symbol-based backward recursion on the root states of the trellis.

Therefore, we start again by substituting the hypothesis for the trellis state $S_n = \sigma_2$ with the associated subset $\mathcal{P}_{\sigma_2}$ of codewords having the same prefix $\mathbf{c}_{[0,...,\sigma_2]}$. Correspondingly, the β term is reformulated as

$$\beta_n(\sigma_2) = p\left(\hat{\mathbf{b}}_{n+1}^N | S_n = \sigma_2, \hat{\mathbf{b}}_1^n\right)$$
$$= p\left(\hat{\mathbf{b}}_{n+1}^N | I_0 \in \mathcal{P}_{\sigma_2}, S_\nu = 0, \hat{\mathbf{b}}_1^n\right) \quad (13)$$

where again, $\nu = n - l(\mathbf{c}_{[0,...,\sigma_2]})$ refers to the bit position of the affected root state $S_\nu = 0$. The expression in (13) can now be decomposed according to

$$\beta_n(\sigma_2) = \frac{1}{C'(\sigma_2)} \sum_{\mu \in \mathcal{P}_{\sigma_2}} p\left(\hat{\mathbf{b}}_{n+1}^N | I_0 = \mu, S_\nu = 0\right)$$
$$\cdot P\left(I_0 = \mu | S_\nu = 0, \hat{\mathbf{b}}_1^n\right) \quad (14)$$

where the sum in (14) is equal to the PDF $p(\hat{\mathbf{b}}_{n+1}^N, I_0 \in \mathcal{P}_{\sigma_2} | S_\nu = 0, \hat{\mathbf{b}}_1^n)$. The normalization factor $C'(\sigma_2)$ is given by

$$C'(\sigma_2) = P\left(I_0 \in \mathcal{P}_{\sigma_2} | S_\nu = 0, \hat{\mathbf{b}}_1^n\right)$$
$$= \sum_{\mu \in \mathcal{P}_{\sigma_2}} P\left(I_0 = \mu | S_\nu = 0, \hat{\mathbf{b}}_1^n\right). \quad (15)$$

Note that the first term in the sum of (14) does not depend on $\hat{\mathbf{b}}_1^n$ anymore, since we condition on a certain quantization index $I_0 = \mu$ starting at the root state $S_\nu = 0$. In the following, let $\nu' = \nu + l(\mathbf{c}(\mu))$ denote the bit position which marks the end of the VLC codeword $\mathbf{c}(\mu)$ of the considered quantization index $I_0 = \mu$, and let $\mathbf{c}_{[\sigma_2,...,0]}(\mu)$ be the postfix of the codeword $\mathbf{c}(\mu)$ starting at the state $S_n = \sigma_2$. The PDF $p(\hat{\mathbf{b}}_{n+1}^N | I_0 = \mu, S_\nu = 0)$, $\mu \in \mathcal{P}_{\sigma_2}$ in (14) can then be written as

$$p\left(\hat{\mathbf{b}}_{n+1}^N | I_0 = \mu, S_\nu = 0\right) = p\left(\hat{\mathbf{b}}_{\nu'+1}^N | I_0 = \mu, S_\nu = 0\right)$$
$$\cdot p\left(\hat{\mathbf{b}}_{n+1}^{\nu'} | \mathbf{c}_{[\sigma_2,...,0]}(\mu)\right) \quad (16)$$

where the channel term $p(\hat{\mathbf{b}}_{n+1}^{\nu'} | \mathbf{c}_{[\sigma_2,...,0]}(\mu))$ contains the soft information at the output of the transmission channel for the codeword postfix $\mathbf{c}_{[\sigma_2,...,0]}(\mu)$ from bit position $(n + 1)$ to ν' associated with the source hypothesis $I_0 = \mu$. Due to the memoryless property of the channel, we obtain

$$p\left(\hat{\mathbf{b}}_{n+1}^{\nu'} | \mathbf{c}_{[\sigma_2,...,0]}(\mu)\right) = \prod_{\eta=1}^{l(\mathbf{c}_{[\sigma_2,...,0]}(\mu))} p\left(\hat{b}_{n+\eta} | c_\eta(\mu)\right) \quad (17)$$

where $c_\eta(\mu)$ denotes the ηth bit of the postfix $\mathbf{c}_{[\sigma_2,...,0]}(\mu)$ and $p(\hat{b}_{n+\eta} | c_\eta(\mu))$ the corresponding channel term, respectively. Furthermore, a similar decomposition to that shown in (9) can be applied to the term $P(I_0 = \mu | S_\nu = 0, \hat{\mathbf{b}}_1^n)$ in (14) and (15), where again, the corresponding normalization factor and the

channel term for the prefix cancel out in (14). Thus, (14) can be reformulated as

$$\beta_n(\sigma_2) = \frac{1}{C''(\sigma_2)} \sum_{\mu \in \mathcal{P}_{\sigma_2}} \underbrace{p\left(\hat{\mathbf{b}}_{\nu'+1}^N | I_0 = \mu, S_\nu = 0\right)}_{=:B(\nu'|\mu,\nu)}$$

$$\cdot p\left(\hat{\mathbf{b}}_{n+1}^{\nu'} | \mathbf{c}_{[\sigma_2,\ldots,0]}(\mu)\right) \cdot P\left(I_0 = \mu | S_\nu = 0, \hat{\mathbf{b}}_1^\nu\right) \quad (18)$$

with $C''(\sigma_2) = P(I_0 \in \mathcal{P}_{\sigma_2} | S_\nu = 0, \hat{\mathbf{b}}_1^\nu)$, which can be computed as a marginal distribution from $P(I_0 = \lambda | S_\nu = 0, \hat{\mathbf{b}}_1^\nu)$ in (11). As we can see from (18), the term $\beta_n(\sigma_2)$ can be expressed as the marginal distribution of the PDF $B(\nu'|\mu,\nu) := p(\hat{\mathbf{b}}_{\nu'+1}^N | I_0 = \mu, S_\nu = 0)$, the channel term for the postfix, and the probabilities for the codewords starting at bit position ν, given in (11). The symbol-based quantity $B(\nu'|\mu,\nu)$ can be regarded as a modified β term, conditioned on the source hypothesis $I_0 = \mu$ and the root state $S_\nu = 0$, and it can be obtained as an index-based recursion exploiting the source-transition probabilities as a priori information, as we will show in the following.

Let $\nu'' = \nu' + l(\mathbf{c}(\lambda)) = \nu + l(\mathbf{c}(\lambda)) + l(\mathbf{c}(\mu))$ now denote the end position of the next codeword $\mathbf{c}(\lambda)$ corresponding to the subsequent quantization index $I_1 = \lambda$ starting at the bit position ν'. When we solely restrict ourselves to the bit positions for the root states $n = \nu, \nu', \nu'', \ldots$, the term $B(\nu'|\mu,\nu)$ can be expressed as a symbol-based backward recursion, according to

$$B(\nu'|\mu,\nu) = \sum_{\lambda=0}^{2^M-1} \underbrace{p\left(\hat{\mathbf{b}}_{\nu''+1}^N | I_1 = \lambda, S_{\nu'} = 0\right)}_{=B(\nu''|\lambda,\nu')}$$

$$\cdot \underbrace{p\left(\hat{\mathbf{b}}_{\nu'+1}^{\nu''}, I_1 = \lambda, S_{\nu'} = 0 | I_0 = \mu, S_\nu = 0\right)}_{=:\Gamma(\lambda,\nu'|\mu,\nu)}. \quad (19)$$

Finally, for the derivation of the term $\Gamma(\lambda,\nu'|\mu,\nu)$, we can take into account that the probability for a symbol transition is independent from the bit position ν, due to the stationarity of the Markov model of the source signal. Correspondingly, $P(I_1 = \lambda, S_{\nu'} = 0 | I_0 = \mu, S_\nu = 0) = P(I_1 = \lambda | I_0 = \mu)$ holds, and we obtain

$$\Gamma(\lambda,\nu'|\mu,\nu) = p\left(\hat{\mathbf{b}}_{\nu'+1}^{\nu''} | I_1 = \lambda\right) \cdot P(I_1 = \lambda | I_0 = \mu). \quad (20)$$

As in the classical BCJR-style backward recursion, the term $\Gamma(\lambda,\nu'|\mu,\nu)$ in (20) contains both a priori source statistics and information from the transmission channel; both the source index-transition probabilities $P(I_1 = \lambda | I_0 = \mu)$ and the soft information $p(\mathbf{b}_{\nu'+1}^{\nu''} | I_1 = \lambda)$ for the source hypothesis $I_1 = \lambda$ at the channel output are used. The latter expression can be calculated by multiplying the corresponding bit-based channel PDFs analog to (17). The desired relation for $\beta_n(\sigma_2)$ in (2) is now obtained by combining (18)–(20).

Now we have all terms available to calculate the APPs $P(b_n = i|\hat{\mathbf{b}})$ from (2) with known quantities, where besides the source statistics, only the number of transmitted bits N is used as side information in the APP computations. Finally, in order to obtain an estimate for the source symbol packets $\hat{\mathbf{I}}$ and $\hat{\mathbf{U}}$, the bit-based APPs $P(b_n = i|\hat{\mathbf{b}})$ are provided as soft-input values to a subsequent VLC sequence estimation. Here, a MAP

estimate $\mathbf{b}_{\mathrm{MAP}} = \arg\max_{\mathbf{b}} \prod_{n=1}^N P(b_n|\hat{\mathbf{b}})$ for $\mathbf{b}$ is sought on the given bit-level trellis, which represents a variable-length encoded version of the estimated index sequence $\hat{\mathbf{I}}$. To obtain $\mathbf{b}_{\mathrm{MAP}}$, the soft-input Viterbi algorithm is applied to the trellis representation from Section II-B with the path metric

$$M_n(\sigma_2) = \max_{i,\sigma_1} \Big\{ P(b_n = i|\hat{\mathbf{b}})$$

$$\cdot P(b_n = i, S_n = \sigma_2 | S_{n-1} = \sigma_1) \cdot M_{n-1}(\sigma_1) \Big\} \quad (21)$$

minimizing the word-error rate. Herein, $P(b_n = i, S_n = \sigma_2 | S_{n-1} = \sigma_1) = 1$ if a trellis branch associated with the bit $b_n = i$ between the states $S_{n-1} = \sigma_1$ and $S_n = \sigma_2$ exists, and $P(b_n = i, S_n = \sigma_2 | S_{n-1} = \sigma_1) = 0$, otherwise. Finally, the estimates $\hat{\mathbf{I}}$ and $\hat{\mathbf{U}}$ are obtained by tracing back the surviving path. Note that the length $\hat{N}$ of the estimates may differ from the length N of the transmitted source packets, due to estimation errors. In this case, symbols are truncated, or dummy symbols are appended in order to ensure that $\hat{N} = N$.

D. Complexity

In the following, we analyze the complexity of the APP decoding algorithm introduced in the previous section, and compare its complexity with the 3-D trellis-based approach presented in [11]. The main contribution to the complexity of the proposed APP VLC decoder, in terms of arithmetic operations, results from the computation of (11) and (19), which use the transition probability for the source symbols $P(I_0 = \lambda | I_{-1} = \mu)$, and which are calculated for each bit position $n \in \{0, \ldots, N\}$. Thus, the complexity increases linearly with the number of transmitted bits N, and quadratically with the size of the symbol alphabet $|\mathcal{I}|$, according to $C_{[\mathrm{II-C}]} = O(N \cdot |\mathcal{I}|^2) = O(K \cdot |\mathcal{I}|^2)$, since K and N are related as $N = \bar{M}_{\mathrm{VLC}} \cdot K$, with the average VLC codeword length $\bar{M}_{\mathrm{VLC}}$. The benefit of the proposed method becomes obvious, when we compare its complexity with the approach from [11]. Here, the Markov property of the source is used within a supertrellis, where the trellis states $S_k = (\lambda, n)$ are given by the hypothesis for the quantization index $I_k = \lambda$, and the hypothesis for the current bit position n. Due to the time-varying nature of the underlying VLC trellis (see [8]), the complexity is given by $C_{[\mathrm{TK03}]} = O(K^2 \cdot |\mathcal{I}|^2)$, which increases quadratically with the number of symbols K. A comparison to $C_{[\mathrm{II-C}]}$ reveals the complexity reduction obtained by the proposed VLC decoder, especially for long source-block lengths K.

III. ITERATIVE DECODING AND EXIT CHARACTERISTICS

In many transmission situations, the implicit source redundancy may not provide enough error protection for the variable-length encoded bitstream. In the following, we therefore additionally consider explicit redundancy from channel codes inserted into the interleaved output of the VLC encoder, which leads to the extended transmission system shown in Fig. 4. Since the encoder configuration is similar to the one for serially concatenated codes [26], however, with the difference that the redundancy provided by the outer channel encoder is replaced with the residual source redundancy, an ISCD strategy may be
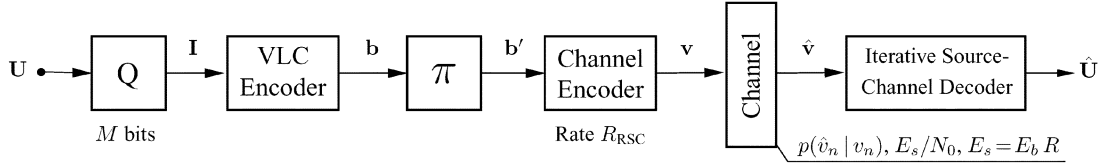
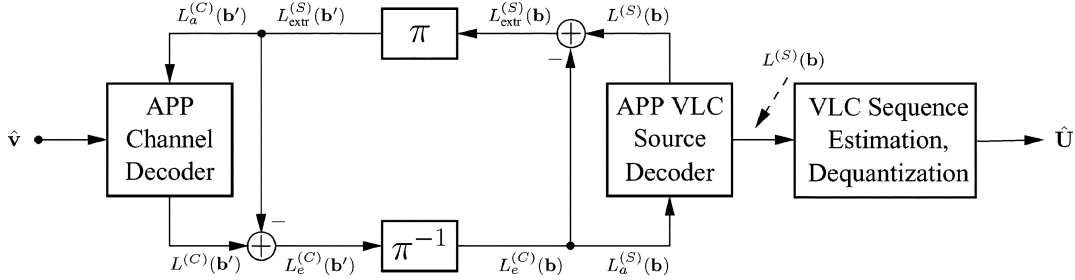Fig. 4.   Extended model of the transmission system.

Fig. 5.   Iterative joint source-channel decoder.

applied. Based on an EXIT chart analysis [23], we optimize the channel code for a given VLC in order to increase the decoding performance, where as the main result, we show that a reliable transmission with RVLCs with a free distance of two and rate-1 systematic convolutional channel codes is possible.

A. Iterative Joint Source-Channel Decoding

Due to the serial concatenation of source and channel encoding, the iterative decoder depicted in Fig. 5 may be used for calculating APPs for the decoded information bits. The decoding is carried out analog to the decoding of serially concatenated channel codes, where the outer constituent decoder is replaced by the APP VLC source decoder derived in Section II-C. In Fig. 5, the (inner) APP channel decoder calculates a posteriori log-likelihood ratios (LLRs) $L^{(C)}(\mathbf{b}')$ for the interleaved information bit vector $\mathbf{b}' = [b'_1, b'_2, \ldots, b'_N]$, where

$$L^{(C)}(b'_n) = \log\left(\frac{P(b'_n = 0|\hat{\mathbf{v}})}{P(b'_n = 1|\hat{\mathbf{v}})}\right)$$

$$L^{(C)}(\mathbf{b}') = \left[L^{(C)}(b'_1), L^{(C)}(b'_2), \ldots, L^{(C)}(b'_N)\right].$$

The LLR $L^{(C)}(b'_n)$ consists of three different components [25], namely, the soft values at the output of the transmission channel $L_c^{(C)}(b'_n)$, the extrinsic values for the information bit $L_{\text{extr}}^{(C)}(b'_n)$, and the a priori values $L_a^{(C)}(b'_n)$. After deinterleaving, the quantity $L_e^{(C)}(\mathbf{b}') = L^{(C)}(\mathbf{b}') - L_a^{(C)}(\mathbf{b}')$ is provided as the soft input $L_a^{(S)}(\mathbf{b})$ to the (outer) APP source decoder, in order to obtain the a posteriori LLRs $L^{(S)}(\mathbf{b})$. Here, the LLRs in $L_a^{(S)}(\mathbf{b})$ contain both the soft values of the transmission channel $L_c^{(C)}(b_n)$ and the extrinsic values $L_{\text{extr}}^{(C)}(b_n)$, which serve as additional a priori information. Correspondingly, the PDFs $p(\hat{b}_n|b_n)$ in Section II-C are replaced by the probabilities associated with the LLRs $L_a^{(S)}(b_n)$. For completing the iteration, the APP source decoder generates the extrinsic values $L_{\text{extr}}^{(S)}(\mathbf{b}) = L^{(S)}(\mathbf{b}) - L_a^{(S)}(\mathbf{b})$, which, after interleaving, can be exploited as additional a priori information $L_a^{(C)}(\mathbf{b}')$ by the inner decoder at the beginning of the next iteration. Finally, using the a posteriori LLRs $L^{(S)}(\mathbf{b})$ as a priori knowledge in

a MAP VLC sequence estimation, as stated in Section II-C, followed by a dequantization leads to an estimate $\hat{\mathbf{U}}$ of the transmitted source sequence $\mathbf{U}$ in each iteration step.

B. EXIT Characteristics and Design of the Iterative Decoding Scheme

In order to analyze the exchange of extrinsic information in the iterative decoding process, we compute EXIT characteristics [23], [27] for the constituent decoders of the iterative source-channel decoder. These characteristics allow us to predict the convergence behavior of the joint decoder, and to find "good" matching pairs of inner and outer codes in order to improve the decoding performance, without simulating the iterative decoder.

The input–output behavior of a SISO decoder can be described by its EXIT characteristic. An EXIT characteristic specifies the relation between the symbolwise mutual information between the transmitted bits b_n and the extrinsic values $L_e(b_n)$ at the output of the decoder, and the symbolwise mutual information between the transmitted bits b_n and the a priori values $L_a(b_n)$ at the input of the decoder. Denoting the mutual information at the a priori input of the inner and outer decoder as I_{A_i} and I_{A_o}, and the mutual information at the extrinsic output of the inner and outer decoder as I_{E_i} and I_{E_o}, given as

$$I_{A_i} = I\left(L_a^{(C)}(b'_n); b'_n\right)$$
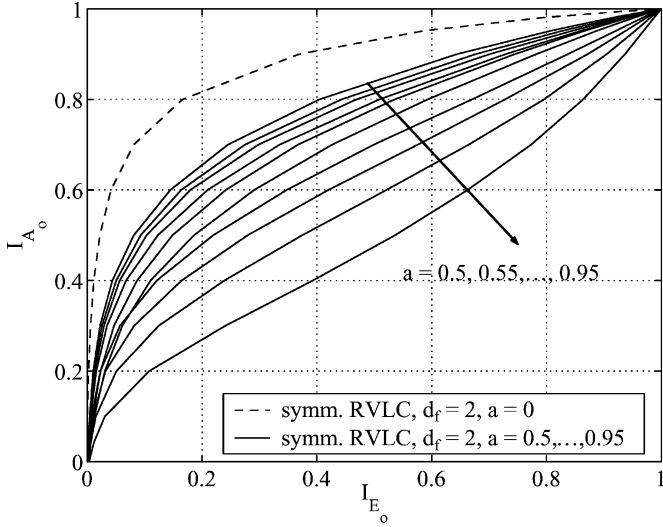
$$I_{A_o} = I\left(L_a^{(S)}(b_n); b_n\right) \tag{22}$$

$$I_{E_i} = I\left(L_e^{(C)}(b'_n); b'_n\right)$$

$$I_{E_o} = I\left(L_{\text{extr}}^{(S)}(b_n); b_n\right) \tag{23}$$

the transfer characteristics T_i and T_o of the inner and outer decoder can be written as

$$I_{E_i} = T_i\left(I_{A_i}, \frac{E_s}{N_0}\right) \quad \text{and} \quad I_{E_o} = T_o(I_{A_o}). \tag{24}$$

Since a priori information and channel observations $\hat{\mathbf{v}}$ are employed in the decoding process of the inner channel decoder, the

Fig. 6. EXIT characteristics (T_o) of the outer APP source decoder.

Fig. 7. EXIT chart of iterative source-channel decoder.

transfer characteristic T_i is parameterized with the channel parameter, e.g., E_s/N_0 in the case of an additive white Gaussian noise (AWGN) channel. For the outer APP source decoder, the a priori information represents the only soft input, such that the transfer characteristic T_o only depends on I_{A_o}. In order to obtain the so-called EXIT chart, both mappings T_i and T_o may now be plotted into one single diagram, where the axes for T_o must be swapped. This is due to the fact that the extrinsic output of the one decoder becomes the a priori input of the other decoder after (de)interleaving (see Fig. 5), and thus, $I_{A_i} = I_{E_o}$ and $I_{A_o} = I_{E_i}$.

Since the source encoder (quantizer and VLC encoder) and the corresponding source statistics represent the given part of the source-channel encoder, we start the analysis with the EXIT characteristic of the outer APP source decoder. In this connection, we restrict ourselves to RVLCs [24], [28], [29], which are simultaneously forward and backward decodable, since their codewords satisfy both the prefix and the suffix conditions. In the following, we use symmetrical RVLCs with free distance $d_f \geq 2$ [13], which are designed by using the method proposed in [29]. This class of codes is especially beneficial for iterative decoding, since the maximal amount of extrinsic information $I_{E_o} = 1$ bit can be obtained for perfect a priori information $I_{A_o} = 1$ bit, due to the distance constraint of the VLC. This can be observed from Fig. 6, where the transfer characteristics $I_{E_o} = T_o(I_{A_o})$ of the VLC source decoder from Section II-C are shown with swapped axes for an AR(1) input process $\mathbf{U}$. In this experiment, we used correlation coefficients $a \in \{0.5, 0.55, \ldots, 0.95\}$, a subsequent uniform quantization with $M = 4$ bits, and a symmetrical RVLC with $d_f = 2$. For the special case where the a priori input is modeled as the outcome of a binary erasure channel (BEC), the area under the transfer characteristic of the outer code with rate R_o is given as $A_o = 1 - R_o$ [30]. Even though this optimal condition is not fulfilled in Fig. 6, where the a priori information is modeled by an appropriate Gaussian noise process [27], our experiments have shown that this area property seems to approximately hold for the transfer characteristic of the APP source decoder, as well.
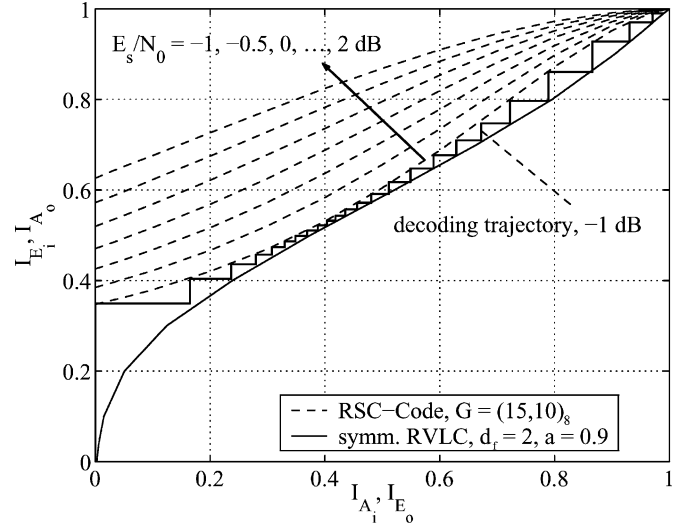
For a certain set of source parameters, we can now use the transfer characteristics T_i and T_o to select an appropriate channel code. Since an intersection of T_i and T_o leads to a fixpoint in the iterative decoding process, each channel code with a characteristic T_i lying above the characteristic T_o of the source decoder may be taken as a matching channel code. For the code design, we use a rate-1 systematic convolutional code, which is obtained by puncturing from a rate-1/2 memory-3 mother code with generator polynomials $(g_0, g_1)_8 = (15, 10)_8$. The code puncturing is performed in such a way that either the information bit b_n or the corresponding parity bit p_n for every $n \in \{1, \ldots, N\}$ is removed from the bitstream. As we can observe from Fig. 7, the channel code obtained by the puncturing pattern

$$\mathbf{P} = \begin{bmatrix} 1 & 0 & 1 & 0 & 1 & 0 & 0 & 1 & 0 & 0 & 1 & 0 \\ 0 & 1 & 0 & 1 & 0 & 1 & 1 & 0 & 1 & 1 & 0 & 1 \end{bmatrix}$$

satisfies the above condition for $E_s/N_0 \geq -1$ dB and a source correlation parameter $a = 0.9$. It is shown in [30] that when a BEC is used as an a priori channel, the area A_i under the transfer characteristic of the inner rate-1 code is given by the capacity of the communication channel, $A_i = C_c$.

In order to visualize the exchange of soft information between the two constituent decoders, a trajectory bounded by the decoder transfer characteristics can be drawn into the EXIT chart. The inner channel decoder starts decoding at $I_{A_i} = 0$ bits and provides extrinsic values with the mutual information $I_{E_i} = T_i(0)$ to the outer source decoder, which now starts decoding at $I_{A_o} = I_{E_i}$. In Fig. 7, the decoding trajectory is obtained from real simulation data for a single block of 20 000 source symbols, and therefore, also takes the increasing correlation between a priori and extrinsic information in further iterations into account. For the above-selected rate-1 RSC code and an $E_s/N_0 = -1$ dB, the simulated trajectory leads to a good convergence behavior, since it is able to pass the bottleneck region. However, this may not generally hold true for other source and channel realizations due to the finite blocklength of the source data. Due to the area properties mentioned above,

the area $(A_i - (1 - A_o))$ between the transfer characteristics for inner and outer codes is related to the gap between the channel capacity C_c and the code rate R_o. Correspondingly, for perfectly matched inner and outer codes, where $(A_i - (1 - A_o))$ tends to zero, and by using an inner code having a rate equal to or larger than one, capacity can be achieved for an infinite block length on a BEC [30]. This motivates the use of rate-1 inner codes.

IV. SIMULATION RESULTS

In this section, simulation results are presented for the ISCD approach from Section III-A, where the VLC APP source decoder proposed in Section II-C is employed as the outer constituent decoder. This scheme is denoted as ISCD-1 in the following, since the first-order Markov property of the source is fully used. The simulations are carried out for an AWGN channel modulated with binary phase-shift keying (BPSK); two correlated sources with $a = 0.5$ and $a = 0.9$, each comprising 20 000 source symbols, uniformly quantized with $M = 4$ bits, and the RVLC from Section III-B are considered. Additionally, we address the case where no *a priori* information is available at the decoder, which is investigated in [13]. We refer to this case as ISCD-0, and the corresponding transfer characteristic T_o is given by the dashed line in Fig. 6. For all configurations, the inner rate-1 code is obtained by appropriate puncturing from a rate-1/2 RSC code with generator polynomials $(g_0, g_1)_8 = (15, 10)_8$, as demonstrated in Section III-B for the case $a = 0.9$.

In order to allow a fair comparison, the channel is parameterized by the signal-to-noise ratio (SNR) E_b/N_0 related to the transmit energy per information bit $E_b = E_s/R$, with E_s denoting the energy per BPSK symbol. The (overall) code rate R for the given system is obtained as

$$R = R_{\text{RSC}} \cdot \underbrace{\frac{H(I_k)}{\bar{M}_{\text{RVLC}}}}_{=:R_{\text{RVLC}}} \cdot \underbrace{\frac{H(I_k|I_{k-1})}{H(I_k)}}_{=:R_{\text{Markov}}} \quad (25)$$

where $\bar{M}_{\text{RVLC}}$ denotes the mean word length after VLC encoding. In (25), R_{RSC} considers the explicit redundancy from the channel encoder, R_{RVLC} the explicit redundancy due to the symmetry condition for the RVLC codewords, and R_{Markov} the implicit residual source redundancy due to the first-order Markov property of the source indexes I_k. The contribution to the overall code rate by the implicit residual source redundancy depends on the correlation coefficient a. Fig. 8 quantifies the connection between R_{Markov} and the correlation coefficient a for the applied Gaussian AR(1) process with a 4-bit uniform quantization. For moderate correlation with $a = 0.5$, the source redundancy can be associated with a code rate $R_{\text{Markov}} = 0.93$, while a high correlation with $a = 0.9$ leads to a code rate $R_{\text{Markov}} = 0.66$. The overall code rates for the three setups are given as $R_{a=0.5} = 0.80$ for correlation coefficient $a = 0.5$, $R_{a=0.9} = 0.57$ for correlation coefficient $a = 0.9$, and $R_0 = 0.86$ in the case where no implicit source redundancy is exploited by the VLC decoder.

Note that the available redundancy per bit is generally given as $1 - R$. Thus, when the rate contribution R_{Markov} from (25)
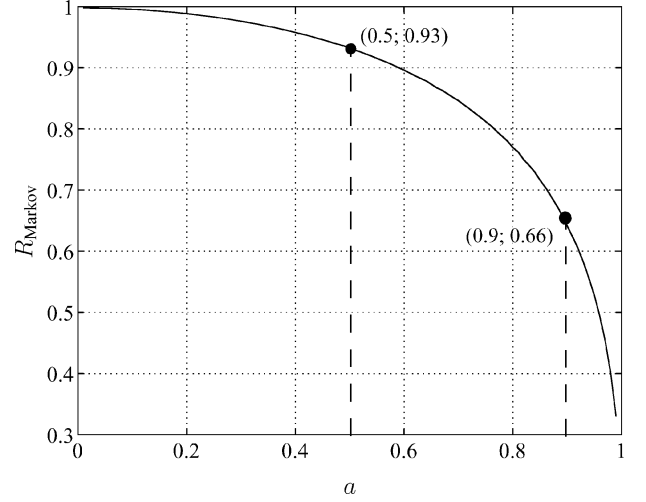

Fig. 8. Amount of redundancy due to a first-order Markov model, in terms of code rate R_{Markov} versus correlation coefficient a for a Gaussian AR(1) process, uniformly quantized with $M = 4$ bits.
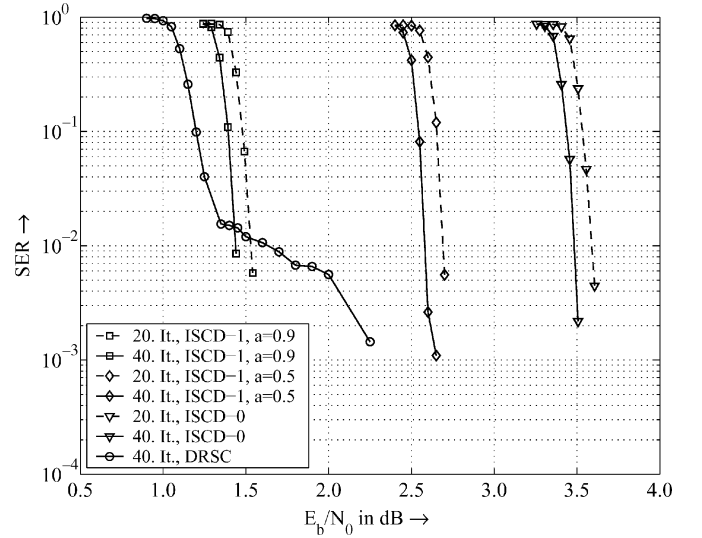

Fig. 9. SER versus E_b/N_0 for the AWGN channel. ISCD for correlated source signals ($a = 0.5$, $a = 0.9$, RVLC with $d_f \geq 2$, ISCD-1), ISCD for uncorrelated source signals (RVLC with $d_f \geq 2$, ISCD-0), and comparison with serial concatenation of a turbo-like code and a Huffman code with instantaneous decoding (DRSC).

is considered, a correlation coefficient of, e.g., $a = 0.9$ for the AR(1) input process leads, according to Fig. 8, to an additional 33% of redundant bits in the frame, compared with only exploiting the source distribution of the indexes I_k. This matches, quite well, the redundancies stated, e.g., for some FS 1016 and MELP speech codec parameters in [17, Table 1] and [18, Table 1], respectively. Therefore, we can conclude that a correlation coefficient of $a = 0.9$ seems to be a reasonable choice for modeling certain parameter correlations in practical source compression systems.

Fig. 9 visualizes the symbol-error rate (SER) obtained by comparison of the estimate $\hat{\mathbf{I}}$ to the transmitted data $\mathbf{I}$ over the channel parameter E_b/N_0. As we can see from Fig. 9, the proposed ISCD-1 approach with correlation coefficient $a = 0.9$ only leads to a negligibly small SER for $E_b/N_0 \geq 1.49$ dB. This is consistent with the decoding trajectory for $E_s/N_0 = -1$ dB

in Fig. 7, where convergence is achieved after 23 iteration steps. Clearly, an increase of the channel SNR leads to a decreasing number of iterations in the waterfall region of the SER–SNR relation. A decrease of the channel SNR leads to a strong increase in SER, where the beginning of the waterfall region corresponds with the intersection of the transfer characteristics for the constituent decoders in the EXIT chart. A similar behavior can be observed when the source correlation is reduced. For a correlation coefficient $a = 0.5$ and for the ISCD-0 method, no transmission errors are observed for $E_b/N_0 \geq 2.7$ dB and $E_b/N_0 \geq 3.7$ dB, respectively.

For comparison purposes, we additionally consider a transmission system comprising a 2-D 6-bit vector quantizer, a Huffman encoder, and a doped repeat scramble code (DRSC) [31] for the AR(1) source with $a = 0.9$. The rate of the DRSC is adjusted to $R_{\mathrm{DRSC}} = 0.56$, which is approximately the rate $R_{a=0.9}$. The decoding of the DRSC is performed iteratively [31], followed by a subsequent VLC sequence estimation. As we can see from Fig. 9, for $E_b/N_0 \leq 1.43$ dB, its SER performance is superior to the proposed ISCD-1 method with $a = 0.9$. However, the achieved reconstruction quality is poor, and thus, this region of channel SNR is not of interest. For $E_b/N_0 > 1.43$ dB, the ISCD-1 method becomes superior, since the DRSC suffers from an error floor at a bit-error rate of approximately 10^{-6}. This comparison shows the good performance of the proposed APP VLC decoding approach as constituent decoder in an iterative joint source-channel decoding scheme, compared with a classical setup, where source and channel decoding is carried out separately.

V. CONCLUSIONS

We have presented a novel VLC APP decoding approach, which can be seen as an extension of the classical bit-based BCJR algorithm adapted to the case of variable-length encoded Markov sources. It exploits the symbol-based source statistics for error concealment, and is based on a simple bit-level trellis representation. This leads to a significant reduction of complexity, compared with previous work, due to the moderate number of trellis states. When considering additional error protection by channel codes, the proposed VLC APP decoder can be applied as constituent decoder for an iterative joint source-channel decoding scheme. The EXIT characteristics of the component decoders show that in the case of RVLCs with distance constraints, a reliable transmission with rate-1 convolutional codes is possible even at low SNR on the transmission channel, when residual source index correlation is present. The simulation results for the AWGN channel verify the good performance of the proposed VLC decoding technique.

ACKNOWLEDGMENT

REFERENCES

[1] V. Buttigieg and P. G. Farrell, "A maximum a-posteriori (MAP) decoding algorithm for variable-length error-correcting codes," in *Codes and Cyphers: Cryptography and Coding. IV.* Essex, U.K.: Institute of Mathematics and Its Applications, 1995, pp. 103–119.

[2] M. Park and D. J. Miller, "Joint source-channel decoding for variable-length encoded data by exact and approximate MAP sequence estimation," *IEEE Trans. Commun.*, vol. 48, no. 1, pp. 1–6, Jan. 2000.

[3] K. Sayood, H. H. Otu, and N. Demir, "Joint source/channel coding for variable-length codes," *IEEE Trans. Commun.*, vol. 48, no. 5, pp. 787–794, May 2000.

[4] A. H. Murad and T. E. Fuja, "Robust transmission of variable-length encoded sources," in *Proc. Wireless Commun. Netw. Conf.*, vol. 2, New Orleans, LA, Sep. 1999, pp. 968–972.

[5] C. Lamy and O. Pothier, "Reduced complexity maximum a posteriori decoding of variable-length codes," in *Proc. IEEE Global Telecommun. Conf.*, vol. 2, San Antonio, TX, Nov. 2001, pp. 1410–1413.

[6] M. Bystrom, S. Kaiser, and A. Kopansky, "Soft source decoding with applications," *IEEE Trans. Circuits Syst. Video Technol.*, vol. 11, no. 10, pp. 1108–1120, Oct. 2001.

[7] L. Perros-Meilhac and C. Lamy, "Huffman tree-based metric derivation for a low-complexity sequential soft VLC decoding," in *Proc. IEEE Int. Conf. Commun.*, vol. 2, New York, NY, May 2002, pp. 783–787.

[8] R. Bauer and J. Hagenauer, "Symbol-by-symbol MAP decoding of variable-length codes," in *Proc. ITG Conf. Source Channel Coding*, Munich, Germany, Jan. 2000, pp. 111–116.

[9] L. R. Bahl, J. Cocke, F. Jelinek, and J. Raviv, "Optimal decoding of linear codes for minimizing symbol error rate," *IEEE Trans. Inf. Theory*, vol. IT-20, no. 2, pp. 287–294, Mar. 1974.

[10] J. Kliewer and R. Thobaben, "Combining FEC and optimal soft-input source decoding for the reliable transmission of correlated variable-length encoded signals," in *Proc. IEEE Data Compression Conf.*, Snowbird, UT, Apr. 2002, pp. 83–91.

[11] R. Thobaben and J. Kliewer, "Robust decoding of variable-length encoded Markov sources using a three-dimensional trellis," *IEEE Commun. Lett.*, vol. 7, no. 7, pp. 320–322, Jul. 2003.

[12] V. B. Balakirsky, "Joint source-channel coding with variable length codes," in *Proc. IEEE Int. Symp. Inf. Theory*, Ulm, Germany, Jun. 1997, p. 419.

[13] R. Bauer and J. Hagenauer, "On variable length codes for iterative source/channel decoding," in *Proc. IEEE Data Compression Conf.*, Snowbird, UT, Mar. 2001, pp. 273–282.

[14] K. Laković and J. Villasenor, "Combining variable length codes and turbo codes," in *Proc. IEEE 55th Veh. Technol. Conf.*, vol. 4, Birmingham, AL, May 2002, pp. 1719–1723.

[15] L. Guivarch, J.-C. Carlach, and P. Siohan, "Joint source-channel soft decoding of Huffman codes with turbo codes," in *Proc. IEEE Data Compression Conf.*, Snowbird, UT, Mar. 2000, pp. 83–92.

[16] A. Guyader, E. Fabre, C. Guillemot, and M. Robert, "Joint source-channel turbo decoding of entropy-coded sources," *IEEE J. Sel. Areas Commun.*, vol. 19, no. 9, pp. 1680–1696, Sep. 2001.

[17] F. I. Alajaji, N. C. Phamdo, and T. E. Fuja, "Channel codes that exploit the residual redundancy in CELP-encoded speech," *IEEE Trans. Speech Audio Process.*, vol. 4, no. 5, pp. 325–336, Sep. 1996.

[18] T. Fazel and T. Fuja, "Robust transmission of MELP-compressed speech: An illustrative example of joint source-channel decoding," *IEEE Trans. Commun.*, vol. 51, no. 6, pp. 973–982, Jun. 2003.

[19] R. Perkert, M. Kaindl, and T. Hindelang, "Iterative source and channel decoding for GSM," in *Proc. IEEE Int. Conf. Acoust., Speech, Signal Processing*, Salt Lake City, UT, May 2001, pp. 2649–2652.

[20] T. Fingscheidt and P. Vary, "Softbit speech decoding: A new approach to error concealment," *IEEE Trans. Speech Audio Process.*, vol. 9, no. 3, pp. 240–251, Mar. 2001.

[21] S. M. Heinen, "An optimal MMSE estimator for source codec parameters using intra-frame and inter-frame correlation," in *Proc. IEEE Int. Symp. Inf. Theory*, Washington, DC, Jun. 2001, p. 237.

[22] T. Fingscheidt, T. Hindelang, R. V. Cox, and N. Seshadri, "Joint source-channel (de-)coding for mobile communications," *IEEE Trans. Commun.*, vol. 50, no. 2, pp. 200–212, Feb. 2002.

[23] S. ten Brink, "Convergence of iterative decoding," *Electron. Lett.*, vol. 35, no. 10, pp. 806–808, May 1999.

[24] Y. Takishima, M. Wada, and H. Murakami, "Reversible variable length codes," *IEEE Trans. Commun.*, vol. 43, no. 2–4, pp. 158–162, Feb.–Apr. 1995.

[25] J. Hagenauer, E. Offer, and L. Papke, "Iterative decoding of binary block and convolutional codes," *IEEE Trans. Inf. Theory*, vol. 42, no. 2, pp. 429–445, Mar. 1996.

[26] S. Benedetto, D. Divsalar, G. Montorsi, and F. Pollara, "Serial concatenation of interleaved codes: Performance analysis, design, and iterative decoding," *IEEE Trans. Inf. Theory*, vol. 44, no. 3, pp. 909–920, May 1998.

[27] S. ten Brink, "Code characteristic matching for iterative decoding of serially concatenated codes," *Ann. Telecommun.*, vol. 56, no. 7–8, pp. 394–408, Jul.–Aug. 2001.

[28] C. W. Tsai and J. L. Wu, "On constructing the Huffman-code-based reversible variable length codes," *IEEE Trans. Commun.*, vol. 40, no. 9, pp. 1506–1509, Sep. 2001.

[29] K. Laković and J. Villasenor, "On design of error-correcting reversible variable length codes," *IEEE Commun. Lett.*, vol. 6, no. 8, pp. 337–339, Aug. 2002.

[30] A. Ashikhmin, G. Kramer, and S. ten Brink, "Extrinsic information transfer functions: Model and erasure channel properties," *IEEE Trans. Inf. Theory*, vol. 50, no. 11, pp. 2657–2673, Nov. 2004.

[31] S. Huettinger, S. ten Brink, and J. Huber, "Turbo-code representation of RA codes and DRS codes for reduced decoding complexity," in *Proc. 35th Annu. Conf. Inf. Sci. Syst.*, Baltimore, MD, Mar. 2001, pp. 118–123.

Ragnar Thobaben was born in Hamburg, Germany, in 1977. He received the Dipl.-Ing. degree in electrical engineering from the University of Kiel, Kiel, Germany, in 2001.

Since October 2001, he has been with the Institute for Circuits and Systems Theory, University of Kiel, as a Research Assistant. His research interests are joint source and channel coding, and iterative source-channel decoding of variable-length encoded source signals.

Mr. Thobaben received the Prof. Dr. Werner Petersen award for his diploma thesis and the award for the best graduation in electrical engineering of the Faculty of Engineering, University of Kiel, in 2001.

Jšrg Kliewer (S'97–M'99–SM'04) received the Dipl.-Ing. degree in electrical engineering from Hamburg University of Technology, Hamburg, Germany, in 1993, and the Dr.-Ing. degree (Ph.D.) in electrical engineering from the University of Kiel, Kiel, Germany, in 1998.

From 1993 to 1998, he was a Research Assistant with the Institute for Circuits and Systems Theory, University of Kiel. In 1996, he spent five months with the Image Processing Lab, University of California, Santa Barbara, as a Visiting Researcher. Since 1999, he has been with the Faculty of Engineering, University of Kiel, as a Senior Researcher and Lecturer. In 2004, he visited the University of Southampton, U.K., for one year, and since 2005, he has been with the University of Notre Dame, Notre Dame, IN, as a Visiting Assistant Professor, on leave from the University of Kiel. His current research interests are in the area of signal processing for communications applications, and include joint source and channel coding, error-correcting codes, and network coding.